Am J Nucl Med Mol Imaging 2021;11(1):27-39
www.ajnmmi.us /ISSN:2160-8407/ajnmmi0123936

Original Article

Physical characteristics of ^{68}Ga DOTATATE PET/CT affecting small lesion detectability

Michael S Silosky[1], Ramesh Karki[1], Rustain Morgan[1], Janet Anderson[2], Bennett B Chin[1]

[1]Department of Radiology, Division of Nuclear Medicine, University of Colorado School of Medicine Anschutz Medical Campus, Aurora, CO, USA; [2]Department of Radiology, Division of Nuclear Medicine, University of Colorado Hospital, University of Colorado Health System, Aurora, CO, USA

Received October 11, 2020; Accepted December 21, 2020; Epub February 15, 2021; Published February 28, 2021

Abstract: Background and purpose: ^{68}Ga DOTATATE PET/CT protocols are similar to ^{18}F FDG protocols despite differences in physical properties, biodistribution, and tumor uptake. The purpose of this study is to evaluate the impact of scan time (counts), and target activity on signal-to-noise ratio (SNR) in various sized targets, or lesions. To evaluate this, phantom experiments and analysis of clinical ^{68}Ga DOTATATE PET/CT studies were performed. Materials and methods: ^{68}Ga was first compared to ^{18}F in phantom studies to evaluate recovery coefficients and SNR. ^{68}Ga phantom studies were also acquired in list mode, and at varying target activities to evaluate the effects of acquisition time and high target concentrations on SNR in clinically relevant small (8 mm) and larger targets (≥ 12 mm). Clinical studies (n = 50) were analyzed to determine if phantom target concentrations and SNR are present in clinical ^{68}Ga DOTATATE studies at similarly very high tumor activity concentrations (n = 159). Results: In phantoms, recovery coefficient and SUV_{max} for ^{68}Ga were ~87% of ^{18}F. SNR for ^{68}Ga was ~65% of ^{18}F. For the ^{68}Ga small target (8 mm) at standard T/B = 2.4, increasing scan time from 5 to 15 minutes increased SNR from < 1 to 1.6, and did not result in target identification. Increasing T/B from 2.4 to 10.9, however, dramatically increased SNR from < 1 to 22.3. Increased T/B resulted in clear visibility of the 8 mm target, even for 1-minute scans. In patients, high hepatic tumor SUV_{max} (27.3±29.6), resulted in high SNR (12.5±9.8). For extrahepatic tumors, high SUV_{max} (41.6±42.8), resulted in high SNR (43.8±49.9). Conclusion: Very high target or T/B, even in small targets, can offset the physical limitations of ^{68}Ga. High target uptake and high T/B are primary factors influencing small lesion detectability.

Keywords: ^{68}Ga, ^{18}F, ^{68}Ga DOTATATE, small lesion, detectability, phantom study

Introduction

Routine oncologic PET/CT imaging of neuroendocrine tumors is primarily performed with ^{18}F fluorodeoxyglucose (FDG). ^{68}Ga DOTATATE imaging protocols are similar to those of FDG PET with an hour uptake period and similar time per bed position [1]. The detectability of small lesions (< 1 cm), however, may be impaired by the physical limitations of ^{68}Ga, including a shorter half-life (68 minutes compared to 110 minutes for ^{18}F), a longer mean free path of the positron, and high energy prompt gamma emissions which could adversely affect random counts and scatter. Compared with FDG, ^{68}Ga DOTATATE imaging typically uses lower injected doses (5 mCi or 185 MBq versus 10 mCi or 370 MBq) [2], and ^{68}Ga DOTATATE has higher normal liver background activity. The combination of reduced counts and physical and biological factors may result in reduced lesion detectability for hepatic tumors, a common site of neuroendocrine metastases.

^{68}Ga DOTATATE, however, has very high receptor affinity to the SSR2, high radiotracer retention, minimal *in vivo* metabolism, and rapid background clearance. Whether or not the current clinical imaging protocols are sufficient for detection of small lesions, particularly relevant in the liver, is unknown.

The purpose of this study is to evaluate several known factors related to small lesion detectability in clinical ^{68}Ga DOTATATE studies. To evaluate the physical properties of ^{68}Ga compared to ^{18}F, and the effect of increasing counts by

Table 1. Phantom dosing information for each scan performed including radionuclide, uptake time, activity concentrations at scanning start time and target-to-background ratio

Scan	Radionuclide	Delay or Uptake (Minutes)	Cylinder Concentration (kBq/ml)	Background Concentration (kBq/ml)	Target to Background Ratio
1	^{18}F	60	4.10	1.74	2.36
2	^{68}Ga	60	3.33	1.40	2.38
3	^{68}Ga	60	14.76	1.36	10.85
4	^{68}Ga	60	30.93	1.37	22.58
5	^{68}Ga	60	48.23	1.36	35.46
6	^{68}Ga	37	4.31	1.74	2.48

increasing imaging time, a series of experiments was performed in phantoms with clinically relevant activity concentrations, imaging times, and test target sizes. To determine if similar activity concentrations (measured by SUV) and SNR measurements are seen in tumors using clinically relevant imaging times and administered activities, a retrospective analysis of clinical ^{68}Ga DOTATATE PET/CT studies was performed. The signal-to-noise ratio (SNR) was used as a metric of lesion detectability [3, 4].

Materials and methods

Phantom data acquisition

First, the imaging characteristics of ^{68}Ga and ^{18}F were compared. An Esser PET phantom (Data Spectrum, Durham NC) was selected because it is a widely available, standard phantom with a well-defined imaging protocol, and structure sizes relevant to this investigation. Also, the standard filling protocol provides activity concentrations commonly seen in clinical ^{18}F FDG studies. This phantom is available in most facilities, and is required by the American College of Radiology (ACR) for accreditation in PET [5]. A series of phantom scans was performed with data acquired and reconstructed using a Gemini TF PET/CT scanner (Philips Medical Systems, Cleveland OH), which has the capability of list mode acquisitions and reconstructions.

Before imaging with ^{68}Ga, a benchmark scan was performed in accordance with the ACR PET Accreditation Program Testing Instructions [5] using ^{18}F and the facility's standard whole body PET/CT protocol. The phantom was dosed in accordance with the ACR testing instructions assuming an administered activity of 185 MBq (5 mCi) because this is typical for ^{68}Ga DOTATATE studies. Activity was assayed using a CRC-55tw (Capintec, Florham Park NJ) dose calibrator. A NIST traceable Ge-Ga standard was used to verify that the ^{68}Ga setting was accurate within 4%. A 60-minute decay period between phantom activity calibration and the scan was used to simulate decay during uptake. Data were acquired for 15 minutes in list mode using a single bed position centered over the hot cylinders. To quantify the effect of scan duration on SNR, images were reconstructed at five different time intervals (1, 1.5, 3, 5 and 15 minutes).

Following the ^{18}F acquisition, several phantom scans were performed using ^{68}Ga. The first scan was performed with the same parameters used for ^{18}F. To evaluate the effects of target-to-background ratio (T/B) on SNR, three additional scans were performed. The background activity concentration was held constant (varying by less than 3%) but the activity concentration in the targets was increased, resulting in higher T/B. A final scan was performed with the standard T/B but a reduced uptake time, compensating for the shorter half-life of ^{68}Ga, to ensure that the activity concentration at the time of scanning was similar to that of the ^{18}F phantom. **Table 1** lists the radionuclide, decay time, activity concentrations at scanning start time, and T/B for each scan. The activity concentration in the background was filled to yield a mean Standardized Uptake Value (SUV_{mean}) of 1.

Phantom reconstruction and data analysis

Phantom images were reconstructed with a 144 × 144 image matrix and a voxel size of 4 mm^3 using Philip's 3D-RAMLA algorithm. Each 15-minute data set was reconstructed in combinations of frames and durations as follows: 15 frames × 1 minute, 10 frames × 1.5 min-

utes, 5 frames × 3 minutes, 3 frames × 5 minutes, and 1 frame × 15 minutes.

For each frame duration, a single reconstructed frame corresponding to the central time point of the scan was analyzed. As an example, when three, 5-minute frames were reconstructed, the second frame was analyzed. Measurements were performed on 5 adjacent slices centered in the axial extent of the hot targets. Circular regions of interest (ROI) were drawn on the CT images with a diameter set to match each target (25 mm, 16 mm, 12 mm, and 8 mm). These ROIs were transferred to the PET images and their positioning was verified. The maximum SUV (SUV_{max}) and mean SUV (SUV_{mean}) were recorded for each ROI. Also, a background ROI was drawn in the center of each slice, with a diameter of 25 mm and SUV_{mean} was recorded. SNR was calculated for each target on each of the five images as:

$$SNR = \left(\frac{\bar{x}_s - \bar{x}_{bg}}{\sigma_{bg}}\right) \quad (1)$$

where $\bar{x}_s$ is the SUV_{mean} of the hot target, $\bar{x}_{bg}$ is the SUV_{mean} of the background, and σ_{bg} is the standard deviation of the background [4]. For each target, the mean SNR and standard deviation were calculated from the SNR from the five slices. Additionally, the recovery coefficient (RC) was calculated for each target for scans 1 and 2. RC was determined as the ratio of the activity concentration measured in each target to the known activity concentration [6]. The paired t-test was used in matched comparisons between ^{18}F and ^{68}Ga that included recovery coefficients, and activity measurements. Differences were considered statistically significant for p values of ≤ 0.05.

Clinical ^{68}Ga DOTATATE PET/CT studies

Clinical ^{68}Ga DOTATATE PET/CT studies (n = 50) were retrospectively analyzed following institutional IRB approval. Patients had been referred for known or suspected neuroendocrine tumors. PET/CT imaging (Discovery ST; GE Healthcare) was performed as follows: intravenous administration of a mean dose of 5.68 mCi (range = 4.3-6.4 mCi) of ^{68}Ga DOTATATE, a mean uptake time of 63.1 minutes (range = 55-81 minutes), and patient voiding prior to scanning. The PET scan was acquired using 5 minutes per bed position, from the mid-thigh to the base of the skull. CT images were acquired from the skull base to mid-thigh and used for attenuation correction and co-localization of PET activity. PET images were reconstructed with OSEM (iterations = 2, subsets = 21) with attenuation and scatter correction and post-reconstruction Gaussian filtering (6 mm FWHM).

Clinical image visualization and analysis were performed on MIM workstations (MIM Encore, and MIM 6.9). For hepatic lesions, background regions were defined by an automated workflow, placing a 3 cm diameter sphere in normal liver, and subsequently verified as normal background by the operator. Lesions were then contoured using a modified PERCIST criteria with a threshold of 1.5 times the SUV_{mean} in the background plus 2 standard deviations. For extrahepatic lesions, background regions were manually placed in the aortic blood pool with contouring and measurement performed using the same methodology as for hepatic lesions. Because the highest background was in the liver, all visually positive hepatic lesions were measured. For extrahepatic lesions, a maximum of 5 lesions with the highest SUV_{max} were measured [7]. All tumor lesions were visually verified as "true" hepatic or extrahepatic metastatic lesions by a board-certified NM radiologist who also verified with the clinical interpretation of the study.

Results

Phantom studies of ^{68}Ga versus ^{18}F-SUV and recovery coefficient

Table 2 lists mean values of SUV_{max} for each phantom scan, target size, and frame duration. The average value of SUV_{mean} of the background ROI for the 3-minute frame duration is also included. SUV_{max} measured using ^{68}Ga was 87.0%±7.1% of that using ^{18}F across all targets and frame durations. This difference was found to be statistically significant ($P < 0.01$). ^{68}Ga SUV was lower than ^{18}F SUV for all but the smallest target size and shortest frame duration where targets were essentially undetectable. The RC for ^{18}F compared to ^{68}Ga as a function of varying target size (scans 1 and 2 from **Table 1**; 15-minute frame duration and T/B of 2.4) are shown in **Figure 1**. As indicated by the reduced SUV_{max} in **Table 2**, the RC for ^{68}Ga was lower than ^{18}F for all target sizes. These results are consistent with previous work reporting reduced RC of ^{68}Ga compared to ^{18}F [6].

Table 2. Measurements of target (SUV_{max}) and background (SUV_{mean}) for all phantom scans and time frame durations described in **Table 1**

Scan Data	^{68}Ga, 60 Min, T/B: 22.58				^{68}Ga, 60 Min, T/B: 35.46				^{68}Ga, 37 Min, T/B: 2.47				^{18}F, 60 Min, T/B: 2.36				^{68}Ga, 60 Min, T/B: 2.38				^{68}Ga, 60 Min, T/B: 10.85			
Background SUV_{Mean}	0.87				0.79				0.80				0.99				0.89				0.87			
Target (mm)	25	16	12	8	25	16	12	8	25	16	12	8	25	16	12	8	25	16	12	8	25	16	12	8
15 minutes	19.44	17.27	12.89	7.01	30.60	26.97	21.44	11.38	2.08	1.75	1.34	0.94	2.42	1.99	1.49	1.16	2.03	1.54	1.30	1.00	9.36	8.43	6.49	3.36
5 minutes	19.38	17.09	12.99	7.06	30.37	26.42	21.28	11.52	2.30	1.79	1.34	1.09	2.62	2.04	1.46	1.24	2.14	1.57	1.43	1.11	9.50	8.48	6.43	3.52
3 minutes	19.52	16.82	13.01	7.20	29.96	26.60	21.14	11.79	2.35	1.67	1.29	1.21	2.52	1.96	1.65	1.40	2.05	1.71	1.42	1.17	9.68	8.46	6.84	3.70
1.5 minutes	19.65	16.65	13.19	6.89	30.55	26.81	21.17	11.53	2.36	1.74	1.40	1.23	2.65	1.87	1.74	1.39	2.24	1.67	1.57	1.31	9.99	8.25	6.98	3.81
1 minutes	19.90	16.87	13.08	7.45	31.04	26.54	20.52	11.51	2.51	2.06	1.41	1.53	2.64	1.94	1.71	1.46	2.68	1.97	1.56	1.46	9.21	7.78	7.45	3.60

Table 3. SNR calculated for each target for all phantom scans and time frame durations

Scan Data	^{68}Ga, 60 Min, T/B: 22.58				^{68}Ga, 60 Min, T/B: 35.46				^{68}Ga, 37 Min, T/B: 2.47				^{18}F, 60 Min, T/B: 2.36				^{68}Ga, 60 Min, T/B: 2.38				^{68}Ga, 60 Min, T/B: 10.85			
Target (mm)	25	16	12	8	25	16	12	8	25	16	12	8	25	16	12	8	25	16	12	8	25	16	12	8
15 minutes	193.47	161.77	116.80	66.29	234.84	193.19	148.41	98.49	13.12	10.91	6.13	1.47	19.75	14.26	6.78	3.78	11.20	7.23	4.84	1.57	87.50	74.83	53.45	32.97
5 minutes	166.37	138.85	101.86	58.52	203.56	164.53	127.40	87.20	8.72	7.66	3.54	1.04	12.26	8.54	3.59	1.39	6.85	4.46	3.08	0.18	56.38	47.66	34.02	22.30
3 minutes	103.14	84.64	62.96	36.55	166.33	136.53	104.87	72.93	10.57	8.27	3.48	1.31	9.16	6.81	5.40	2.09	5.77	4.13	2.65	0.05	40.63	33.69	25.71	16.72
1.5 minutes	93.45	75.33	56.33	31.08	98.93	82.21	61.91	42.54	5.71	4.69	1.84	1.78	4.89	3.61	2.37	0.29	3.76	2.49	1.28	0.38	32.73	26.35	20.80	14.04
1 minutes	53.93	44.78	33.23	19.83	106.18	86.23	65.87	44.62	5.13	5.29	0.78	1.47	3.74	2.56	1.51	-0.69	3.63	2.49	1.43	-0.50	21.15	16.53	15.07	8.67

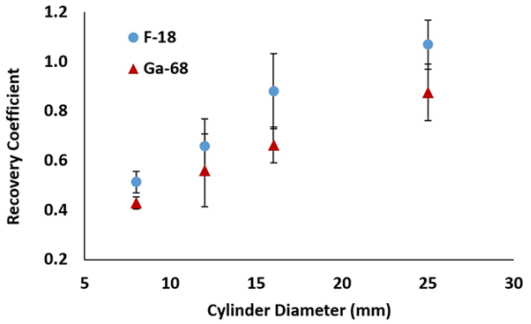

Figure 1. Plots of the recovery coefficients for ^{18}F and ^{68}Ga at a target-to-background ratio (T/B) of approximately 2.40 as a function of target size. Error bars represent the 95% confidence intervals. The recovery coefficients for ^{68}Ga are on average, 87% those for ^{18}F. This difference was found to be statistically significant ($P < 0.01$).

Phantom studies of ^{68}Ga versus ^{18}F-Signal to noise ratio

Table 3 lists mean values of SNR for each phantom scan, target size and frame duration. SNR measured from ^{68}Ga scans was typically lower at 64.7%±29.2% that of ^{18}F scans. **Figure 2A** through **2D** plot SNR as a function of frame duration for the ^{18}F and ^{68}Ga scans using identical scan parameters. As expected, the SNR was higher for the ^{18}F scans for many lesion sizes and frame durations. For example, when the isotope dependent component of spatial resolution is better with ^{18}F compared to ^{68}Ga (due to shorter mean free path of the positron), the adverse effect of reduced peak activity from partial volume effect (PVE) is expected to be reduced, or mitigated. For ^{18}F compared to the ^{68}Ga, a higher signal is expected to be detected by ^{18}F, and thus, comparable ^{18}F scans would be expected to show higher SNR. This was shown in many comparable lesion sizes and for comparable scan durations. The exceptions are in cases where the SNR is low for both radionuclides; notably, this is seen in the 1-minute and 1.5-minute frames for the 8 mm lesion, where noise is relatively very high compared to signal (**Figure 2A**). In these cases, SNR for ^{68}Ga was not significantly lower, showing large overlap in the error bars. As the size of the targets increases, mitigating the partial volume effect, the detected target activity increases and the SNR increases to levels where a significant difference in SNR is apparent between ^{68}Ga and ^{18}F (**Figure 2D**).

Figure 3 shows the five consecutive slices used for SNR calculation for the 15-minute frame duration using ^{18}F (top row), ^{68}Ga with 60 minutes between dose measurement and scan (middle row) and ^{68}Ga with 37 minutes between dose measurement and scan (bottom row). Importantly, this shows the effect of target concentration in the clinically relevant T/B ratio of 2.4. Focusing on the small targets, it should be noted that the 8 mm target is visible in some but not all of the ^{18}F images (SNR = 3.78±1.61), and is not visible in any of the ^{68}Ga images (SNR = 1.57±0.83). As mentioned, the reduced time between dosing and scan (bottom row) was used to account for the shorter half-life of ^{68}Ga. Consequently, activity concentrations at the time of scan in the top ^{18}F row and bottom ^{68}Ga row are similar (please see **Table 1**). Regardless, the small 8 mm ^{68}Ga targets cannot be visualized in the bottom row, using 15-minute scan at a clinically relevant 2.4 T/B.

Phantom studies of ^{68}Ga-effects of target size, imaging time, and target concentration on SNR

Figure 4A through **4D** show SNR as a function of target size using ^{68}Ga. The imaging times and target sizes for each T/B are shown. To illustrate the relationship between SNR and experimental visual observations, phantom images from five consecutive slices used in the SNR calculations for ^{68}Ga scans using 1 minute of imaging time are shown (**Figure 5**). The relationship between SNR and lesion size shows a very predictable correlation that is well characterized by quadratic functions (**Figure 4**; R^2 ranging from 0.97 to 0.99). **Figure 4A** shows that at relatively low target concentrations (T/B = 2.4), small targets (8 mm) all have relatively low SNR (< 2), despite relatively long imaging times of 15 minutes. This is concordant with the experimental observation that these small targets could not be visualized using 15 minutes of imaging time (**Figure 3**, bottom 2 rows). **Figure 4A** also shows that at relatively low target concentrations (T/B = 2.4), the larger targets (16 mm or greater) all have relatively high SNR (≥ approximately 5) at 15 minutes of imaging time. Similarly, this is concordant with the experimental observation that all of the larger targets were clearly visualized using 15 minutes of imaging time (**Figure 3**; bottom 2 rows).

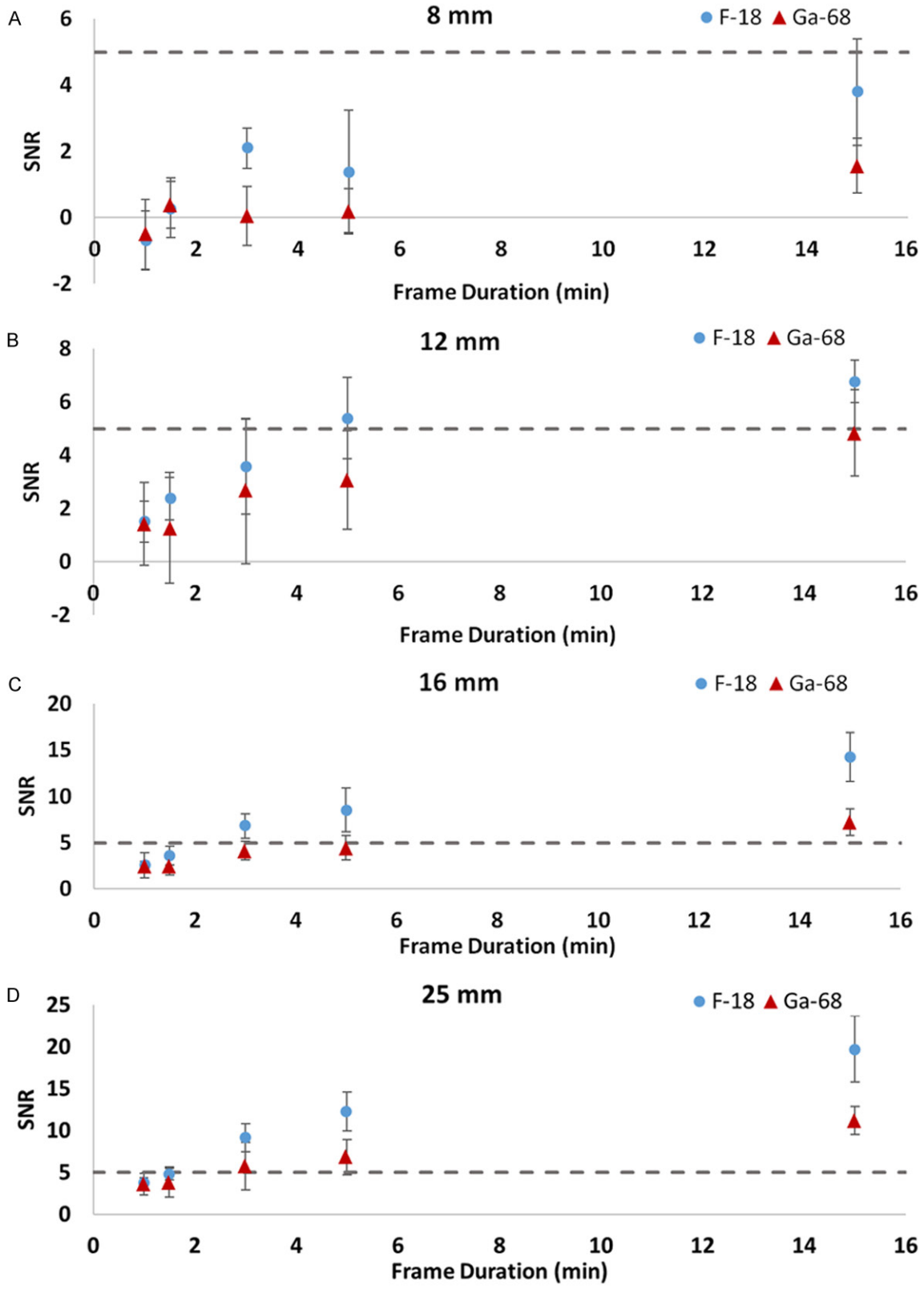

Figure 2. A-D. Signal-to-noise ratio (SNR) is plotted as a function of frame duration for both ^{18}F and ^{68}Ga at a target-to-background ratio (T/B) of 2.4. A-D. Represent target sizes 8 mm, 12 mm, 16 mm, and 25 mm, respectively. Error bars represent a single standard deviation. The dashed line indicates an SNR equal to 5.

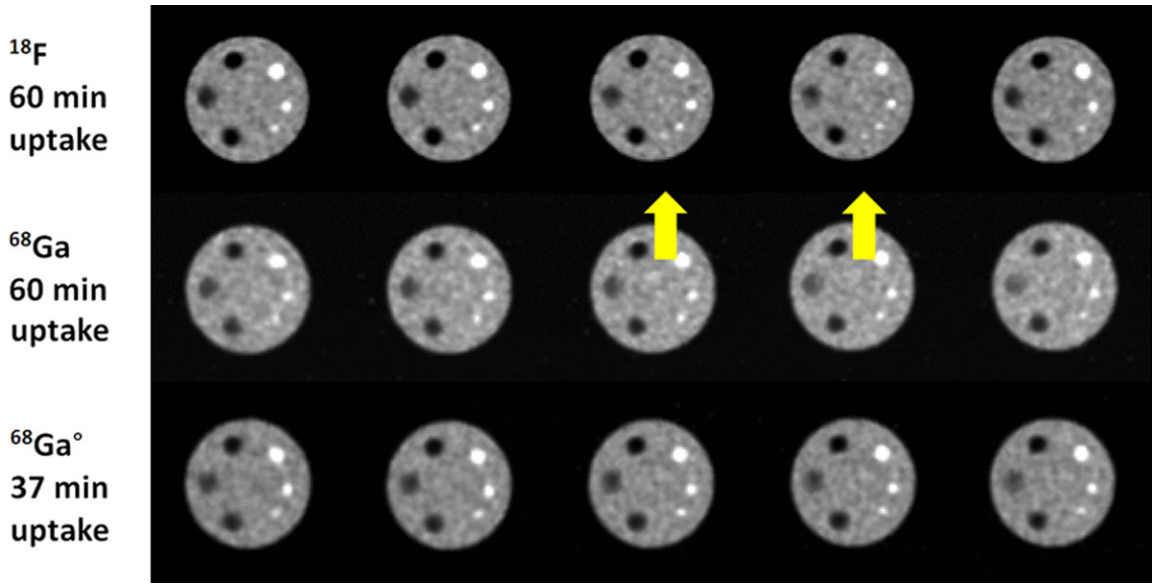

Figure 3. Five consecutive slices used for signal-to-noise ratio calculation for the 15-minute frame duration are displayed for phantom scans using ^{18}F with a 60-minute uptake (top row), ^{68}Ga with a 60-minute uptake (middle row) and ^{68}Ga with 37-minute uptake (bottom row). Window width and level have been adjusted to maintain the brightness of the background activity while attempting to best visualize the hot targets. The reduced uptake time in the last row ensured that activity concentration was similar to that of ^{18}F during scanning. Note that while the smallest target (8 mm) was visible in some slices of the ^{18}F scan as indicated by the arrows, that target cannot be seen in either of the ^{68}Ga scans.

The effect of higher target concentrations on SNR is shown in **Figure 4B** through **4D**. At concentrations ≥ 10.85, the SNR was in all cases greater than 5. This applies to all time imaging time points and all target sizes, including small targets of 8 mm. Focusing on the target concentration of 10.85 (**Figure 4B**), the small target (8 mm) demonstrated SNR of ≥ 5 for all imaging times including the shortest imaging time of 1 minute. This is concordant with the experimental observation that all targets including the small target (8 mm) could be visualized at the shortest imaging time of 1 minute (**Figure 5**, bottom 3 rows).

These results show the dramatic potential impact of high target concentrations, the high T/B, on SNR and lesion detectability despite the modest limitations of ^{68}Ga compared to ^{18}F. To determine if these results might be clinically relevant to ^{68}Ga DOTATATE PET/CT, patient studies were retrospectively evaluated for target or lesion activity.

^{68}Ga DOTATATE PET/CT studies

The demographics of our study population are shown in **Table 4**. Of the 50 patients, 42 showed abnormal ^{68}Ga DOTATATE tumor uptake; 8 patients were negative. Hepatic metastases were most common with sites including abdomen (32 including nodes, abdominal masses, and liver), liver (22), thorax (12), head and neck (9), and bone (3).

Normal background biodistribution and tumor uptake

The normal background SUV_{mean} and SUV_{max} values for ^{68}Ga DOTATATE in the liver (n = 50) were 5.0±1.4 and 8.2±2.8, respectively. Background blood pool values in the aorta (n = 50) were relatively low with SUV_{mean} and SUV_{max} measuring 1.1±0.35 and 1.7±0.70, respectively.

Hepatic tumors (n = 101) were identified with high average SUV_{max} values of 27.3±29.6 (median = 18.5; range = 4.8-223.4). These high tumor uptake values resulted in high mean SNR of 12.5±9.8 (median = 9.3; range = 4.6-71.6), with a corresponding tumor/background of 6.9±9.8 (median = 4.2; range 1.7-82.7). An example is shown in **Figure 6**.

Extrahepatic tumor (n = 58) uptake values were also very high with an average SUV_{max} of 41.6±42.8 (median = 32.4; range = 8.4-301.9).

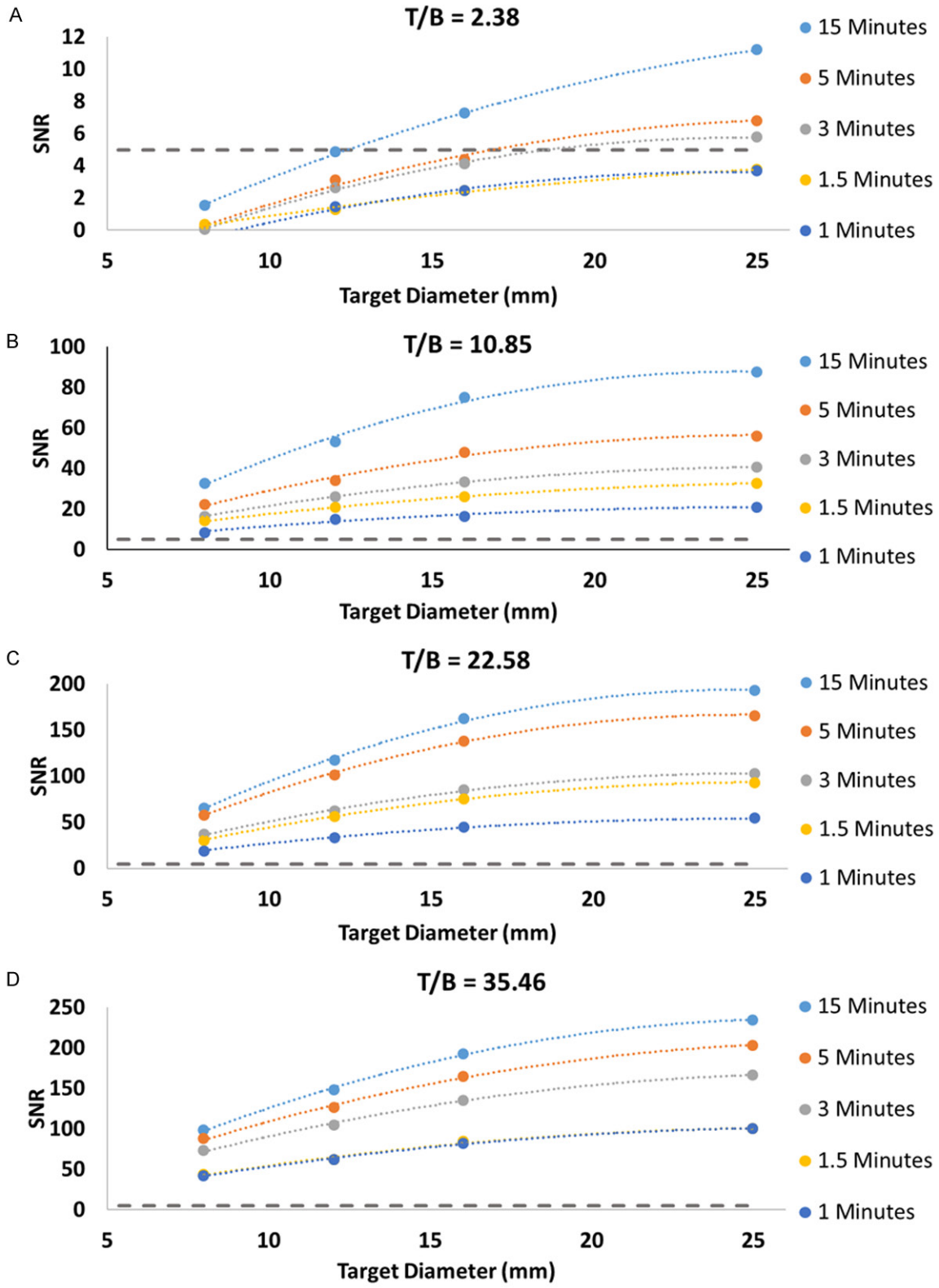

Figure 4. A-D. Plot signal-to-noise ratio (SNR) as a function of target diameter for each frame duration at each target-to-background ratio (T/B) for ^{68}Ga. This relationship was well fit with quadratic functions with values of R^2 ranging from 0.97 to 0.99. The dashed line indicates an SNR equal to 5. Increases in T/B resulted in exceptional improvement in SNR.

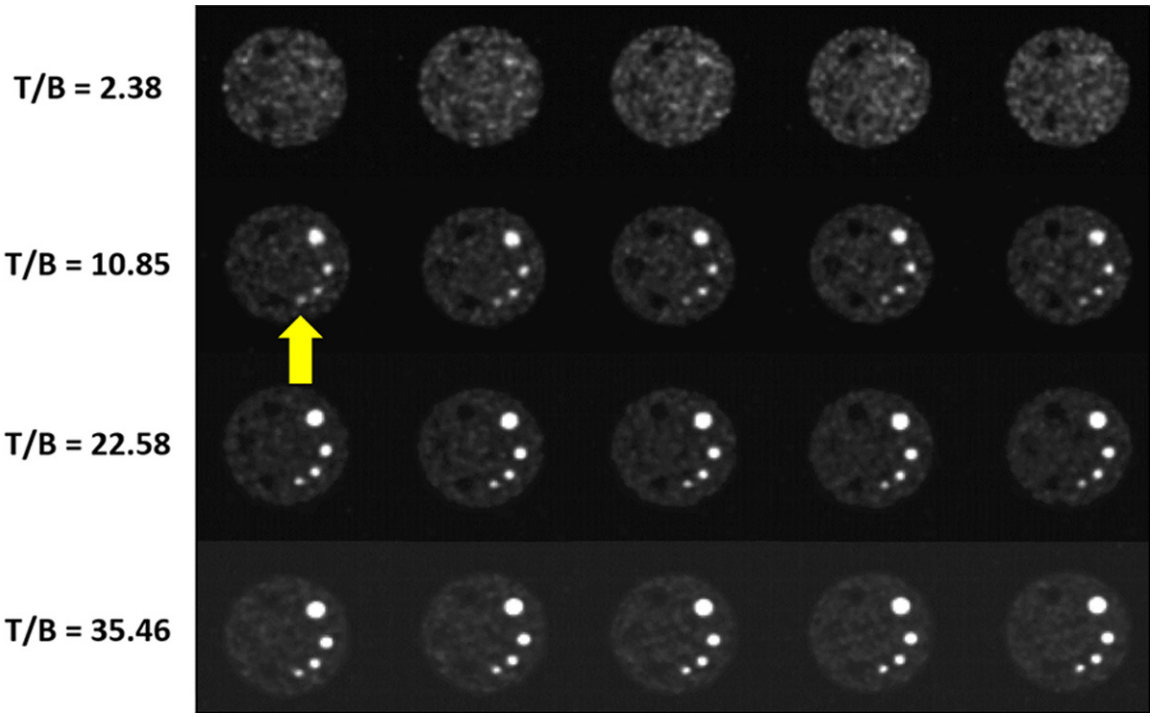

Figure 5. Five consecutive slices used for signal-to-noise ratio calculation for the 1-minute frame duration are displayed for phantom scans using ^{68}Ga. Window width and level has been adjusted to maintain the brightness of the background activity while attempting to best visualize the hot targets. Target-to-background ratio (T/B) increases from 2.38 in the top row to 35.46 in the bottom row. It should be noted that at the lowest target-to-background ratio, the hot targets are practically indistinguishable from background. At even the second lowest ratio, 10.85, even the smallest target (8 mm) is visible in each image (arrow).

Table 4. Patient demographics and baseline characteristics

Parameter	Value
Mean age (years)	60 (16)
Women	59 (16)
Men	61 (16)
Sex (no. of patients)	
Women	21 (42)
Men	29 (58)
Primary Tumor Site	
Small bowel	15 (30)
Pancreas	14 (28)
Large Bowel	7 (14)
Head and Neck	3 (6)
Lung	2 (4)
Retroperitoneal	1 (2)
None (normal scans)	8 (16)
Ki 67	
Low/Intermediate (< or = 20%)	20 (40)
High grade (> 20%)	2 (4)
No Pathology Report	28 (56)

Note-Values in parentheses are percentages, except for age (Standard Deviation).

These high tumor uptake values resulted in high SNR of 43.8±49.9 (median = 28.9; range = 7.9-245.3). The corresponding mean tumor/background blood pool was 44.5±52.8 (median = 28.9; range = 6.1-314.5). In a carotid body tumor, an exceptionally high SUV_{max} of 301.9 was measured.

Discussion

This study evaluates the physical properties of ^{68}Ga compared to ^{18}F to assess their relative contributions to signal-to-noise ratio, a metric of lesion detectability. Phantom studies at standard concentrations (T/B = 2.4) compared ^{68}Ga to ^{18}F, and demonstrated that the recovery coefficient was adversely affected. The relative degree of reduction in RC (~87% of ^{18}F), however, was modest. These results are very similar to a recent report for ^{68}Ga with recovery coefficients reduced by approximately 20% using a clinical PET-CT scanner [6]. Also, SNR was consistently lower for ^{68}Ga than for ^{18}F with an average reduction of 35%. Concordant with these measurements, visual target detectability for ^{68}Ga was reduced, making

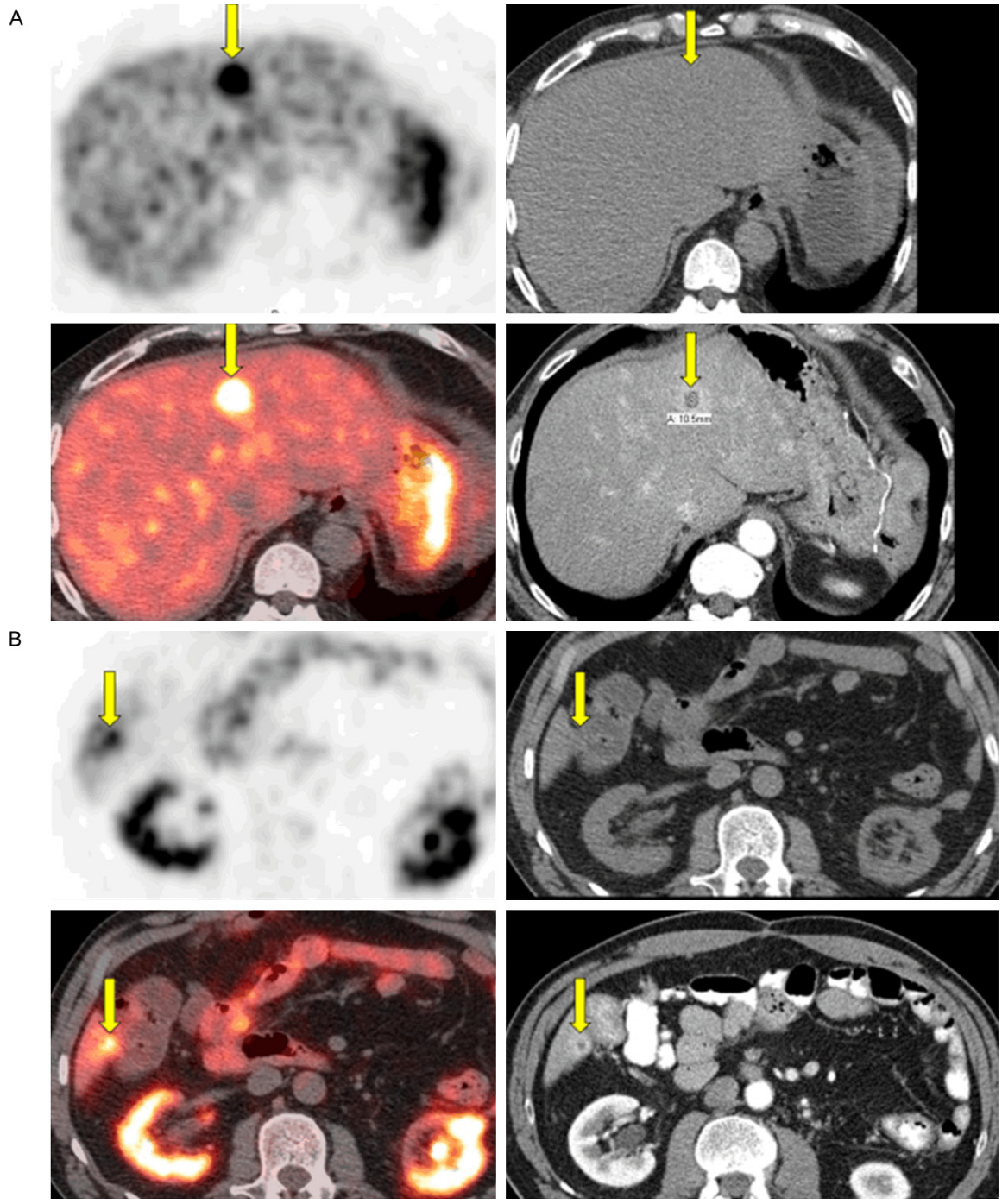

Figure 6. 59-year-old male with primary pancreatic neuroendocrine tumor and liver metastases detected on ^{68}Ga DOTATATE images. Background liver activity SUV_{mean} 5.6. A. (top left) Transaxial PET shows a relatively large focus of ^{68}Ga DOTATATE intense uptake (SUV_{max} 23.5; SNR = 11.0; T/B = 4.2); (top right) Concurrent non-contrast study shows no CT correlate; (bottom left) PET fusion images with concurrent non-contrast CT; (bottom right) contrast enhanced CT performed 3 months later demonstrates moderate sized arterial phase enhancing lesion (11 mm). B. (top left) Transaxial PET shows a relatively small focus of ^{68}Ga DOTATATE with modestly intense uptake (SUV_{max} 10.3; SNR = 5.2; T/B = 1.8); (top right) concurrent non-contrast enhanced CT shows no CT correlate; (bottom left) PET fusion images with concurrent non-contrast CT; (bottom right) contrast enhanced CT performed 3 months later demonstrates relatively small arterial phase enhancing lesion (6 mm).

the 8 mm target undetectable at T/B of 2.4, despite the relatively low noise and sufficient counting statistics of the 15-minute scan imaging duration.

When comparing counting statistics of ^{68}Ga DOTATATE to ^{18}F FDG using approximate clinical doses, the lower administered dose and shorter half-life results in an approximately 60% reduction in counts. Our phantom studies show that for small (8 mm) targets that have mild uptake (SUV = 2.4), an increase in counts from increasing imaging time would not result in a significant improvement in SNR. Increasing imaging time by 300% (5 minutes to 15 minutes) only increased SNR from < 1 to 1.6, with the 8 mm targets remaining undetectable. Using the same background concentration, increasing the target concentration from 2.4 to 10.9 resulted in a dramatic improvement in SNR from < 1 to 22.3. The 8 mm targets were then visible with a 5-minute frame duration, and remarkably, also visible at the shortest imaging time of 1 minute (SNR = 8.7). This indicates that increasing target concentration can offset the physical limitations of ^{68}Ga, as well as the reduced counting statistics of ^{68}Ga DOTATATE (reduced injected dose and shorter half-life compared to ^{18}F FDG).

Relating this phantom data to clinical ^{68}Ga DOTATATE PET studies, very high target concentrations or very high tumor uptake may dramatically contribute to SNR, and thus, improve lesion detectability. Our analysis of hepatic tumors confirmed a high mean tumor/background ratio of 6.9±9.6 and a high SNR of 12.5±9.8; extrahepatic tumors showed even higher tumor/background of 44.5±52.6 and SNR 43.8±49.9.

Although many factors influence lesion detectability, SNR was selected as a suitable metric as it is practical and has been used for many years [3]. In an early study by Rose [8], the SNR threshold for detectability of an object was suggested to be “in the neighborhood of 5”. Since then, a variety of alternative detectability indices and observer models have been proposed, and many have shown good correlation with human observer results [9, 10]. Recently, a study evaluating lesion detectability for low dose FDG PET/CT in lung cancer screening protocols compared human observers to a numerical observer model [11]. Clinical lesion detectability was numerically modelled, and it was well correlated with lesion SNR.

More recently, a human observer study evaluated ^{18}F lesion detectability in phantoms [4]. The SNR was calculated for spheres of different diameters (range = 4-15 mm) and different contrast ratios (T/B range = 1.85-15). This study used 5 different PET/CT imaging systems (Philips Gemini-TF, Philips Vereos, GE Discovery 710, Siemens Biograph mCT, and Siemens HRRT), and could not detect small diameter (7.87 mm) spheres under similar conditions (T/B = 1.85:1; 4 × 4 × 4 mm voxel reconstruction; 16 minutes acquisition time). Using the same parameters for all systems, increasing the contrast ratio to 15:1 resulted in improved lesion detectability of even the smallest diameter spheres (range = 4-5 mm). For all systems, the lesions detected by human observers correlated well with SNR of approximately 5 or higher [4]. Although an in-depth evaluation with human observers was not performed for our study, our clinically detected hepatic and extrahepatic lesions all showed a SNR > 4.6. Our study was also notably different compared to the prior report which reported results for ^{18}F, in contrast to our study which reports results for ^{68}Ga. We believe that this is important to validate specifically with ^{68}Ga, due to the potential development of new ^{68}Ga radiotracers with lower administered doses, such as ^{68}Ga PSMA.

The high ^{68}Ga DOTATATE tumor uptake in this study is comparable to results from prior reports [12, 13]. Lesions were categorized as hepatic or extrahepatic because the liver is the most common, and a very difficult site to detect metastatic neuroendocrine tumors. In our study, the average hepatic tumor uptake (SUV_{max} = 27.3±29; n = 101) was similar to a previous report (SUV_{max} = 28.7; n = 15), however, our average hepatic tumor to background ratios were higher (6.9±9.6; n = 101) than previously reported (2.76; n = 21) [12]. This is at least partially attributable to our lower normal background liver uptake as measured by both SUV mean (SUV_{mean} = 5.0±1.4) and SUV_{max} (SUV_{mean} = 7.2±2.6) compared to the prior report (SUV_{max} = 9.12±3.64) [12]. Our study found that normal mean hepatic ^{68}Ga DOTATATE uptake (SUV_{mean} = 5.0±1.4) is approximately twice the normal background mean hepatic uptake of ^{18}F FDG (SUV_{mean} = 2.5±0.6) [14, 15]. Clinically, our hepatic tumor to background ratio and SNR were very high, and concordant with expected values based on the phantom studies.

For extrahepatic tumors, the mean ^{68}Ga DOTATATE tumor uptake was very high (SUV_{max} = 41.6±42.8; range = 8.4-301.9; n = 58),

although lower than previously reported (SUV_{max} = 65.4±47; range = 6.9-244; n = 847) [13]. The difference in SUV may be attributed to differences in patient tumor heterogeneity [16, 17], tumor burden, or other unknown factors. The low extrahepatic background also contributes to the high T/B and SNR. A previous ^{68}Ga DOTATATE study reported mean T/B of 10.7, 39.3, and 37.2 for tumors found in lymph nodes, brain, and bone respectively [12].

The very high tumor uptake of ^{68}Ga DOTATATE in SSR2 positive neuroendocrine tumors is likely attributable to the favorable ligand binding properties reported by Reubi [18]. Ga-DOTA-[Tyr^3]-octreotate was shown to have subnanomolar affinity for the human subtype 2 somatostatin receptor (IC_{50} = 0.2±0.04 nM), superior in performance compared to the other 20 ligands tested [18]. This radioligand also possesses highly desirable biological properties in humans including receptor-ligand complex internalization, integrated uptake over time, lack of *in vivo* metabolism, and rapid background washout via renal excretion. These properties favor high lesion detectability by contributing to high tumor uptake, and low background activity.

The phantom study provides evidence that the small lesion detectability is possible despite suboptimal physical imaging characteristics of ^{68}Ga compared to ^{18}F, if the target activity and T/B are sufficiently high. Our clinical studies show that ^{68}Ga DOTATATE tumor uptake in neuroendocrine tumors is frequently very high resulting in high T/B, and thus, this is a primary attribute contributing to small lesion detectability.

This study had several limitations. Phantom experiments were performed on a single PET/CT system. In a similar phantom study using 5 different modern PET/CT scanners, SNR amongst different scanners was very comparable, and in agreement with findings from our study [4]. Each PET/CT manufacturer and their specific scanners have differences in instrumentation, acquisition protocols, and software reconstructions which influence the lesion detectability. Our study identified the relative effects of differences between ^{68}Ga compared to ^{18}F, activity concentration (T/B), and imaging time on SNR for small (8 mm) and larger (≥ 12 mm) targets. The precise magnitude of these differences will vary with specific systems, and thus, the threshold at which small lesions can be detected will depend on the specific performance of the system as well as the below described clinical factors.

SNR is relatively easy to calculate, has been used as a metric of detectability, and correlates with human observer studies [11]. One factor that was not investigated was the effect of count rate on SUV and SNR. High count rates may substantially affect the rate of random events, potentially resulting in a loss of image contrast. These effects are less likely because the phantom activity concentrations are similar to those seen in clinical studies.

Many clinical and patient specific factors cannot be not incorporated into the phantom studies that affect SNR. Some factors include biologic variability in tumors which may have lower SSR2 expression [16, 17], coexistent patient medical conditions such as renal failure, patient respiratory motion, variability in body habitus (variability in attenuation, and scatter), and other factors which may lead to decreased tumor uptake and false negative results. The intent of examining the clinical studies, however, was to provide supporting evidence that lesion detectability based on SNR from the phantom studies could be seen in clinical practice, and that this is relevant to clinical ^{68}Ga DOTATATE imaging. Finally, this retrospective study could not measure hepatic metastases due to the lack of IV contrast in most studies. A prospective study with a dedicated liver protocol measuring small lesions would provide more definitive evidence to confirm small lesion detectability.

In conclusion, high target activity and high T/B have a tremendous impact on SNR, a primary metric of lesion detectability. High target concentrations and high T/B can overcome the modest reduction in SNR due to the suboptimal physical properties of ^{68}Ga compared to ^{18}F, and lower counts (due to lower administered activity and shorter half-life), and can ultimately result in overall high SNR. The biodistribution and tumor uptake properties of the ^{68}Ga DOTATATE ligand (very high receptor affinity, radiotracer internalization, minimal in vivo metabolism, and rapid renal excretion) favor very high tumor uptake and high T/B which result in overall high SNR. High tumor uptake

and high T/B are primary factors influencing small lesion detectability.

Disclosure of conflict of interest

None.

Address correspondence to: Michael S Silosky, Department of Radiology, Division of Nuclear Medicine, University of Colorado Anschutz Medical Campus. Mail Stop C278, 12700 East 19th Avenue, Aurora, Colorado 80045, USA. Tel: 303-724-3760; Fax: 303-724-3795; E-mail: Michael.Silosky@ucdenver.edu

References

[1] Hope TA, Bergsland EK, Bozkurt MF, Graham M, Heaney AP, Herrmann K, Howe JR, Kulke MH, Kunz PL, Mailman J, May L, Metz DC, Millo C, O'Dorisio S, Reidy-Lagunes DL, Soulen MC and Strosberg JR. Appropriate use criteria for somatostatin receptor PET imaging in neuroendocrine tumors. J Nucl Med 2018; 59: 66-74.

[2] Subramaniam RM, Bradshaw ML, Lewis K, Pinho D, Shah C and Walker RC. ACR practice parameter for the performance of gallium-68 DOTATATE PET/CT for neuroendocrine tumors. Clin Nucl Med 2018; 43: 899-908.

[3] Burgess AE. The rose model, revisited. J Opt Soc Am A Opt Image Sci Vis 1999; 16: 633-646.

[4] Adler S, Seidel J, Choyke P, Knopp MV, Binzel K, Zhang J, Barker C, Conant S and Maass-Moreno R. Minimum lesion detectability as a measure of PET system performance. EJNMMI Phys 2017; 4: 1-14.

[5] American College of Radiology. American College of Radiology PET accreditation program testing instructions. 2018.

[6] Sanchez-Crespo A. Comparison of Gallium-68 and Fluorine-18 imaging characteristics in positron emission tomography. Appl Radiat Isot 2013; 76: 55-62.

[7] Pinker K, Riedl C and Weber WA. Evaluating tumor response with FDG PET: updates on PERCIST, comparison with EORTC criteria and clues to future developments. Eur J Nucl Med Mol Imaging 2017; 44: 55-66.

[8] Rose A. The sensitivity performance of the human eye on an absolute scale. J Opt Soc Am 1948; 38: 196-208.

[9] Wangerin KA, Ahn S, Wollenweber S, Ross SG, Kinahan PE and Manjeshwar RM. Evaluation of lesion detectability in positron emission tomography when using a convergent penalized likelihood image reconstruction method. J Med Imaging (Bellingham) 2017; 4: 011002.

[10] Barrett HH, Yao J, Rolland JP and Myers KJ. Model observers for assessment of image quality. Proc Natl Acad Sci U S A 1993; 90: 9758-9765.

[11] Schaefferkoetter JD, Yan J, Sjoholm T, Townsend DW, Conti M, Tam JK, Soo RA and Tham I. Quantitative accuracy and lesion detectability of low-dose (18)F-FDG PET for lung cancer screening. J Nucl Med 2017; 58: 399-405.

[12] Kuyumcu S, Ozkan ZG, Sanli Y, Yilmaz E, Mudun A, Adalet I and Unal S. Physiological and tumoral uptake of (68)Ga-DOTATATE: standardized uptake values and challenges in interpretation. Ann Nucl Med 2013; 27: 538-545.

[13] Sadowski SM, Neychev V, Millo C, Shih J, Nilubol N, Herscovitch P, Pacak K, Marx SJ and Kebebew E. Prospective study of 68Ga-DOTATATE Positron emission tomography/computed tomography for detecting gastro-enteropancreatic neuroendocrine tumors and unknown primary sites. J Clin Oncol 2016; 34: 588-596.

[14] Chin BB, Green ED, Turkington TG, Hawk TC and Coleman RE. Increasing uptake time in FDG-PET: standardized uptake values in normal tissues at 1 versus 3 h. Mol Imaging Biol 2009; 11: 118-122.

[15] Boktor RR, Walker G, Stacey R, Gledhill S and Pitman AG. Reference range for intrapatient variability in blood-pool and liver SUV for 18F-FDG PET. J Nucl Med 2013; 54: 677-682.

[16] Bodei L, Ambrosini V, Herrmann K and Modlin I. Current concepts in 68Ga-DOTATATE imaging of neuroendocrine neoplasms: interpretation, biodistribution, dosimetry, and molecular strategies. J Nucl Med 2017; 58: 1718-1726.

[17] Charoenpitakchai M, Liu E, Zhao Z, Koyama T, Huh WJ, Berlin J, Hande K, Walker R and Shi C. In liver metastases from small intestinal neuroendocrine tumors, SSTR2A expression is heterogeneous. Virchows Arch 2017; 470: 545-552.

[18] Reubi JC, Schar JC, Waser B, Wenger S, Heppeler A, Schmitt JS and Macke HR. Affinity profiles for human somatostatin receptor subtypes SST1-SST5 of somatostatin radiotracers selected for scintigraphic and radiotherapeutic use. Eur J Nucl Med 2000; 27: 273-282.